

Influence of Metal Identity on Light-Induced Switchable Adsorption in Azobenzene-Based Metal-Organic Frameworks

Hannah F. Drake,^{a,b} Zhifeng Xiao,^b Gregory S. Day,^{a,b} Shaik Waseem Vali,^c Luke L. Daemen,^a Yongqiang Cheng,^a Peiyu Cai,^b Jason E. Kuszynski,^b Hengyu Lin,^b Hong-Cai Zhou^{b,d,*} and Matthew R. Ryder^{a,e*}

- a. Neutron Scattering Division, Oak Ridge National Laboratory, Oak Ridge Tennessee 37831, United States of America
- b. Department of Chemistry, Texas A&M University, College Station, Texas 77843, United States of America
- c. Department of Biochemistry and Biophysics, Texas A&M University, College Station, Texas 77843, United States of America
- d. Department of Materials Science, Texas A&M University, College Station, Texas 77843, United States of America
- e. Materials Science and Technology Division, Oak Ridge National Laboratory, Oak Ridge Tennessee 37831, United States of America

Keywords: Metal-Organic Frameworks, Gas Storage, Photoresponsive Materials, Light-Induced Switchable Adsorption, Coordination Chemistry, Energy Storage

ABSTRACT: Energy-efficient capture and release of small gas molecules, particularly carbon dioxide (CO₂) and methane (CH₄) are of significant interest in academia and industry. Porous materials such as metal-organic frameworks (MOFs) have been extensively studied, as their ultra-high porosities and tunability enable significant amounts of gas to be adsorbed while also allowing for specific applications to be targeted. However, because of the microporous nature of MOFs, the gas adsorption performance is dominated by high uptake capacity at low pressures, limiting their application. Hence, stimuli-responsive materials, particularly light-induced switchable adsorption (LISA), offer a unique alternative to thermal methods. Here, we report the mechanism of a well-known LISA system, the azobenzene-based material PCN-250, for CO₂ and CH₄ adsorption. There is a noticeable difference in the LISA effect dependent on the metal cluster involved, with the most significant being PCN-250-Al, where the adsorption can change by 83.1% CH₄ and 56.1% CO₂ at 298 K and 1 bar and inducing a volumetric storage change of 36.17 cm³/cm³ and 33.9 cm³/cm³ at 298 K between 5-85 bar (CH₄) and 2-9 bar (CO₂), respectively. Using UV-light in both single-crystal X-ray diffraction and gas adsorption testing, we show that upon photoirradiation, the framework undergoes a 'localized heating' phenomenon comparable to an increase of 130 K for PCN-250-Fe and improves the working capacity. This process functions because of the constrained nature of the ligand, preventing the typical trans-to-cis isomerization observed in free azobenzene. In addition, we observed that the degree of localized heating is highly dependent on the metal cluster involved, with the series of isostructural PCN-250 systems showing variable performance based upon the degree of interaction between the ligand and the metal center.

Introduction

The utilization of highly porous materials for small-molecule gas capture is of significant interest because of the large quantity of gas that can be adsorbed onto the high surface areas of the framework structures.¹⁻⁵ Porous materials, such as metal-organic frameworks (MOFs), have a rich history,⁶ and are particularly well known for their ordered structures involving organic linkers and metal nodes, both of which allow for a high degree of tunability. The structural control of MOF materials allows for the surface areas to be modified and enables tailored functionalization towards desired applications. This typically involves tuning the selectivity towards a specific molecule in gas adsorption.⁷⁻¹⁰

Methane (CH₄) is a significant component of natural gas and therefore of interest as a possible fuel source for the commercial power and heat sectors and an essential feedstock chemical. There is also a growing interest in the transportation sector because CH₄ emits less carbon dioxide (CO₂) per unit of energy than existing gasoline-burning automobiles. Hence, the U.S. Department of Energy (DOE) has

established target metrics for deliverable capacities of CH₄, specifically in the transportation sector. These targets include a gravimetric storage capacity of 0.5 g g⁻¹ and a volumetric capacity of 263 cm³ STP cm⁻³ within the 5-85 bar pressure range.¹¹⁻¹² Although there are candidate MOF materials that meet the initial uptake requirement (total amount of gas adsorbed), the deliverable working capacity (usable amount of gas in the desired pressure range), remains limited, with the first candidate to meet volumetric and gravimetric performance goals only recently being reported.¹³ Many porous materials have a significant amount of their uptake capacity filled well below the minimum pressure of 5 bar described in the DOE guidelines. Hence, making a portion of the adsorbed gas unusable in deliverable capacity.¹⁴ Candidate systems with a high total gas uptake and a high deliverable working capacity, therefore, remain somewhat elusive.

Because of the highly porous nature of MOF materials, there are many examples of total gas uptakes well above the

minimum desired storage threshold.^{4,14} However, the maximum uptake of the material often does not translate to a correspondingly high deliverable working capacity (essentially the difference in uptake at the maximum and minimum usable pressures). Many materials have low working capacities despite their significantly high gas uptakes.¹³⁻¹⁹ A variety of approaches have been proposed to overcome this issue, including breathable materials,²⁰⁻²² monolithic superstructures,²³ and stimuli-responsive systems.²⁴⁻²⁵ Due to the rapid advances in modern light-emitting diode technology, as well as the precise tunability of light stimuli-responsive structures, there has been a general increase in interest in utilizing photoirradiation to combat the gas delivery dilemma in ultra-porous materials.²⁶ Light as a stimuli-responsive trigger is advantageous because it can be engineered into a variety of systems, is readily abundant, and is often more cost-effective than other stimuli-responsive technique strategies. Additionally, it is a strategy that is incorporated into other scaffolds.²⁷

A promising light-responsive functional group, azobenzene, has been reported in several robust MOF systems for diverse applications.²⁸⁻³¹ Azobenzene in free solution undergoes a trans-to-cis isomerization in the presence of UV light. The photo-induced isomerization of the molecule is caused by the $\pi \rightarrow \pi^*$ electronic transition.³² Additionally, the molecule can be easily functionalized to precisely tune the wavelength maximum of absorbance for this transition.^{28, 33-34} Hence, framework materials with azobenzene incorporated into their structures, either as a guest (Type 1),³⁵⁻³⁶ a pendent group (Type 2),^{33, 37-39} or as a part of the linker backbone (Type 3),⁴⁰⁻⁴¹ can undergo light-induced switchable adsorption (LISA) of guest molecules at tunable wavelengths. In Type 1 and 2 systems, the photo-induced gas release is triggered by the isomerization of the azobenzene moiety in the framework. However, in Type 3 systems, the azobenzene moiety serves as the backbone of the framework, and consequently, the isomerization is restricted. Despite the inability to isomerize, a strong LISA effect was observed and confirmed in such a system, which has implied an unknown alternative pathway to trigger gas release.^{25, 40} We hypothesized that the LISA effect in a Type 3 system is caused by the vibrational relaxation of the excited states of the azobenzene moiety under light radiation. The electronic structures of the ligand are often critically affected by the metal identity, as the metal Lewis acidity and metal-ligand charge transfer effect can largely shift the electronic structures of the ligand. Investigation into metal influence on the Type 3 LISA effect can aid in revealing the underlying mechanism as well as in designing light-responsive gas

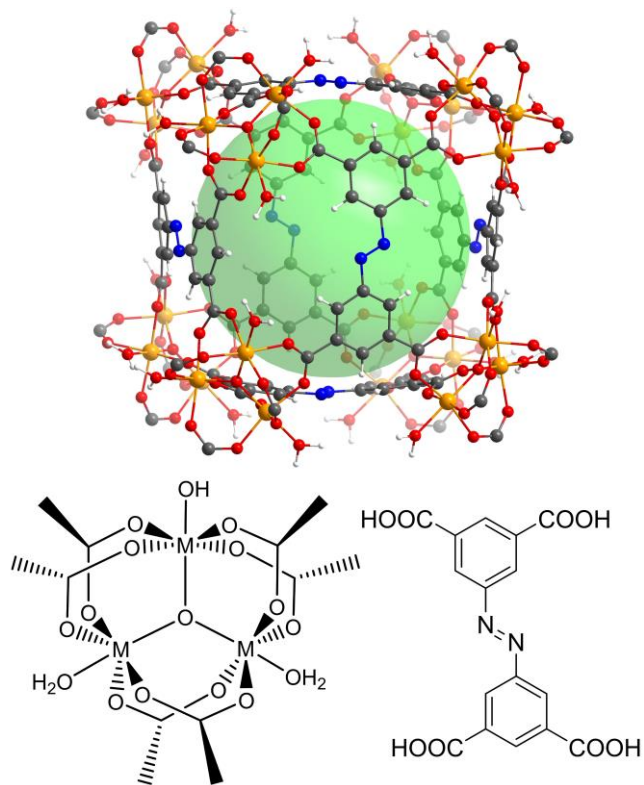


Figure 1. Structure of PCN-250-M, and the metal cluster where $M = \text{Fe}, \text{Al}, \text{In}, \text{or Sc}$, and the H₄ABTC ligand.

adsorbents. Herein, we examine the LISA effects of an azobenzene-based, isoreticular series of MOFs, known as PCN-250 (also called MIL-127),⁴² to elucidate the mechanism of scaffold-based Type 3 LISA systems in CO₂ and CH₄ adsorption and release (Figure 1).

Results and Discussion

A series of isoreticular MOFs derived from 3,3',5,5'-azobenzene tetracarboxylic acid (ABTC) were synthesized and confirmed to be isomorphic using powder X-ray diffraction (PXRD). The powder patterns, N₂ isotherms, and porosity measurements matched well with previous reports (shown in the supporting information).⁴³⁻⁴⁶ In the analogs of PCN-250-M, where $M = \text{Sc}_3, \text{Al}_3, \text{and In}_3$, (also called In-soc-MOF-1a, Sc-ABTC/socMOF, and Al-soc-MOF-1d),^{43, 45, 47-48} the structures do not undergo a thermal generation of open metal sites.⁴³ However, we previously reported that PCN-250-Fe could undergo thermal decarboxylation under standard activation conditions, resulting in open metal sites.⁴⁹ Therefore, to avoid the influence of open metal site

Table 1: BET surface areas, and CH₄ and CO₂ adsorption data at 273 K and 298 K for each of the PCN-250 structures.

| PCN-250 | BET surface area (m ² /g) | 273K CO ₂ adsorption (cm ³ /g STP) | 298K CO ₂ adsorption (cm ³ /g STP) | 273K CH ₄ adsorption (cm ³ /g STP) | 298K CH ₄ adsorption (cm ³ /g STP) |
|--------------------------|--------------------------------------|--|--|--|--|
| Fe ₃ (II/III) | 1,619 | 133.66 | 74.10 | 27.78 | 22.43 |
| Fe ₃ (III) | 1,598 | 50.81 | 37.07 | 16.04 | 11.18 |
| Al ₃ | 1,874 | 170.48 | 106.10 | 43.70 | 34.01 |
| Sc ₃ | 1,321 | 101.31 | 83.62 | 30.85 | 20.01 |
| In ₃ | 1,224 | 108.15 | 69.13 | 25.72 | 16.93 |

Note: CO₂ and CH₄ adsorption at 1 bar.

formation and to provide an accurate comparison between the isomorphs, the Fe-based material was also activated under supercritical CO₂.⁵⁰ The unactivated and supercritical CO₂-activated PCN-250-Fe structures were investigated using ⁵⁷Fe Mössbauer spectroscopy, which is sensitive to the oxidation state and ligand environment of the ⁵⁷Fe nuclei. The spectra of both the unactivated and supercritical CO₂ activated samples at 5 K were dominated by a quadrupole doublet (~80% spectral intensity) with isomer shift $\delta = 0.50 \pm 0.02$ mm s⁻¹ and quadrupole splitting ΔE_Q ranging from 0.55 to 0.65 mm s⁻¹. The spectra also contained a sextet at 5 K (~20% spectral intensity), which collapsed into the doublet at 150 K, similar to previous observations.⁴⁹ These results indicate that the Fe atoms in both the unactivated and supercritical CO₂-activated materials are primarily Fe^{III}. For comparison, the thermally activated sample produces a mixed valent Fe^(II)Fe^(III)₂ cluster.⁴⁹

To our knowledge, only the thermally activated PCN-250-Fe structure (containing μ_3 -oxo Fe₃^(II/III) activated clusters) has been investigated regarding the LISA effect, so it was of interest to include the supercritical CO₂ obtained analog in the current study.⁴⁰

Gas Sorption Analysis of the LISA Effect

The N₂ adsorption isotherms at 77 K for all PCN-250 structures (Al₃, Sc₃, In₃, and Fe₃) show a steep increase in the low-pressure region and a flattened portion at pressures above 0.1 p/p^o characteristics of Type 1 gas sorption curves.⁵¹ The results are consistent with the microporous nature of the

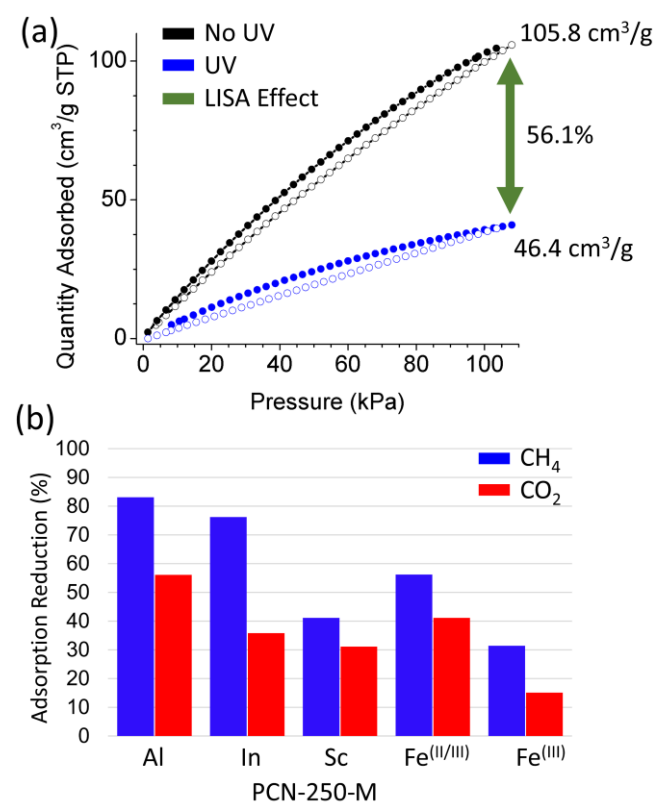


Figure 2. (a) CO₂ sorption isotherms at 298 K for PCN-250-Al showing the gas uptake with and without UV light. (b) The reduction in adsorption (%) at 298 K is shown for CH₄ and CO₂ for all isomorphs.

materials. The BET surface areas are reported in Table 1 along with the 273 K and 298 K CO₂ and CH₄ adsorption uptake at 1 bar.

It is well documented that derivatives of azobenzene experience photoisomerization under light irradiation close to their adsorption maxima.³² It has also been reported that PCN-250-Fe^(II/III) has adsorption maxima at 335 nm and 370 nm,⁵² thus, the utilization of UV light at 374 nm was sufficient to trigger the photoresponse as the adsorption corresponds to the dominant transition for these systems. Upon continuous light irradiation during adsorption, it was observed that the gas uptakes for all five isomorphs were significantly reduced, but to different extents depending on the identity of the metal involved. The reduction in adsorption at 1 bar for each structure with CO₂ and CH₄ at 298 K is reported in Figure 2b, and the additional values at 273 K are included in the supporting information (Table S1). The findings show that PCN-250-Fe^(II/III), the version of the Fe₃ activated thermally and containing high open metal site content,⁴⁹ are consistent with literature reports for CO₂ at 298 K.⁵² For each structure, the LISA effect was higher with CH₄ than CO₂. The M₃^(III) isomorphs in order of the effect for both gasses were Al > In > Sc > Fe. The trend of Fe₃^(II/III) > Fe₃^(III) for both CH₄ and CO₂ adsorption also indicates that redox activity and availability of electronic energy with open metal sites in the isoreticular system may be significant. The difference between the uptakes of the system in both Fe₃ variants (Table 1) may be attributed to the availability and presence of open metal sites. The difference may also be explained by the orbital availability of the metals involved in their ionic and coordination bonding character. Additionally, as the primary electronic transition is $\pi \rightarrow \pi^*$ under UV, there is potential for metal interaction with the excited state due to the symmetry of the orbitals. This is especially interesting as the trend is inversely proportional to the expected potential metal-ligand interaction with the system in terms of bonding character. Therefore, the finding that the LISA effect depends on the metal identity in these isostructural systems could be significant.

High-pressure adsorption was conducted at 298 K on the top-performing material, PCN-250-Al, to test for usability towards the high-pressure storage of CO₂ and CH₄ in line with the DOE goals for the corresponding pressure ranges. The initial uptake performance of PCN-250-Al towards CH₄ was 0.17 g/g and 165.92 cm³/cm³ at 90 bar and 298 K, while CO₂ was 0.49 g/g and 175.72 cm³/cm³ at 9 bar and 298 K. We utilized a custom-built high-pressure UV-irradiation cell to test the sample (discussed in the supporting information). The system allowed us to expose the material to UV light through the bottom of the chamber. The LISA effect on the high-pressure working capacity (amount of usable gas that can be delivered from the MOF within a desired pressure range) was determined to be 22.3% for CH₄ at the DOE range of 5-85 bar, and 22.1% for CO₂ at 2-9 bar (Figure 3). These results equate to a change in CH₄ gravimetric storage of 0.04 g/g and volumetric storage of 36.17 cm³/cm³ for 5-85 bar, and 0.03 g/g and 33.9 cm³/cm³ between 2-9 bar for CO₂ (a table of each value is included in the supporting information as table S2). Additional high-pressure adsorption measurements, IR studies, and PXRD assessments were performed on the samples after each UV experiment, with

additional tests showing no loss in performance compared to the initial adsorption tests (Figures S12-13, S20, S21, S29-32). Pressure cycling also indicated no loss in performance for each sample tested (Figures S23 and S24). This indicated that the change in performance seen in the UV experiments resulted from the UV irradiation and not due to irradiation-induced degradation. Therefore, although the PCN-250 materials do not meet the desired deliverable working capacities outlined by the DOE, the results provide a promising approach towards future research directions in the field of science-driven carbon capture and methane storage.

Single Crystal Diffraction and Neutron Scattering

Under UV irradiation, azobenzene can go through trans-to-cis isomerization in solution. Meanwhile, in PCN-250, the azobenzene-based ligands are constrained by multiple strong bonds. Therefore, we hypothesize that the UV radiation absorbed by the ligand is dissipated thermally through vibrational relaxation. Therefore, the localized increased vibrational amplitude caused by UV radiation results in 'localized heating', causing gas desorption around the N=N bond. We investigated the amplitude and vibrational nature of the framework material and azobenzene-based ligand under UV irradiation to demonstrate the mechanistic hypothesis. Single-crystal X-ray diffraction (SCXRD) obtained on Beamline 12.2.1 was used to probe the increased vibrational amplitude and atomic displacements of the azobenzene-based ligand. SCXRD studies were conducted on a crystalline sample of PCN-250-Fe under N_2 flow at varying temperatures using a custom UV-irradiation setup at the Advanced Light Source (ALS) beamline 12.2.1. In crystallography, anisotropic displacement parameters (ADPs) describe the

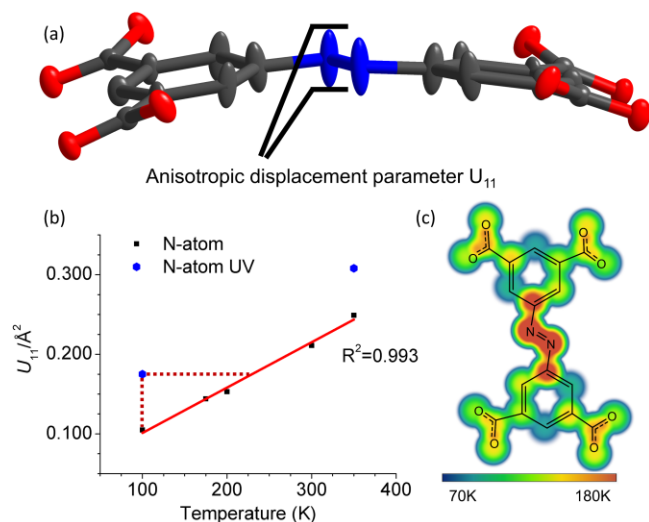


Figure 4. (a) Ellipsoid model of the azobenzene-based ligand in PCN-250-Fe under UV irradiation at 100 K. The atomic displacement parameter (ADP), U_{11} , represents the thermal displacement perpendicular to the ligand plane as depicted by the elongated ellipsoids. (b) Calibration curve of U_{11} with respect to temperature for the nitrogen atoms showing the displacement parameter for both the 100 K and 350 K sample under UV in blue. (c) Temperature map of the ligand under photoexcitation conditions at 100 K as extrapolated from the calibration curves of the U_{11} parameter of each atom.

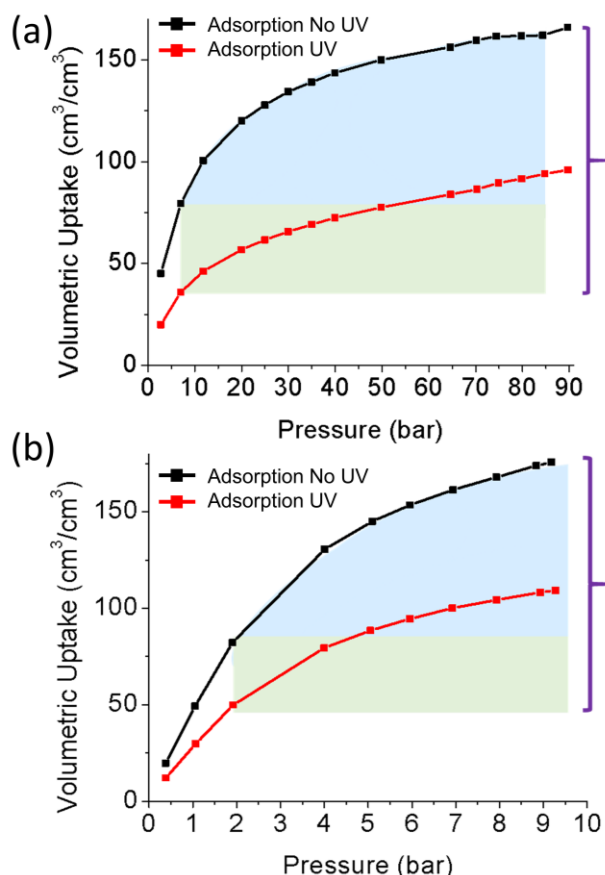


Figure 3. High-pressure adsorption at 298 K of PCN-250-Al with (red) and without UV (black) UV-irradiation for (a) CH_4 at 0-90 bar and (b) CO_2 at 0-10 bar. The working capacities of the system in range of 5-85 bar (CH_4) and 2-9 bar (CO_2) under standard conditions (blue) and the additional working capacity under UV (green) are shown. The total working capacity for a LISA system is highlighted by the purple bar to the right of each graph, which is the addition of the blue and green regions.

thermal motions of the scattering centers in different directions, as depicted by the widely used ellipsoid atomic model (Figure 4a). Here, the ADPs of the ligand atoms in the structure are measured and compared to correlate with the vibrational amplitude of the atoms in the framework. Specifically, one of the ADPs, U_{11} , represents the thermal displacement of the atoms perpendicular to the ligand plane as the thermal displacements within the ligand plane are primarily constrained by the framework.

As shown in the refinement results in the supporting information, the U_{11} values of the azobenzene nitrogen atoms increase by about 0.7 \AA^2 under UV radiation at both 100 K and 350 K, while the atoms in the metal clusters show no noticeable changes in U_{11} values, which supports the UV-induced localized heating effect. To correlate the changes in U_{11} values with temperature, a linear calibration curve for non-irradiated U_{11} in terms of temperature was developed from datasets obtained from the same crystal. The R^2 value for the calibration curve fitting of the anisotropic displacement parameter U_{11} was high for all atoms on the ligand, with a value of $R^2 = 0.993$ observed for the nitrogen atoms

in the azobenzene unit (Figure S25-28 and Table S3). With the linear calibration curves parameters, the U_{11} for different atoms on the ligand under UV light at 100 K is converted into temperature values and visualized in a two-dimensional heat map of the ligand (Figure 4c). Localized temperature increases of approximately 130 K were observed in the proximity of the azo bond unit at both 100 K and 350 K. Mechanistically speaking, the localized heating effect results from the UV-irradiation, which causes direct heating primarily to the azobenzene N=N bond. Due to the significant extinction coefficient of the azobenzene unit, the energy input from the light radiation has high efficiency of conversion into molecular thermal energy.

Inelastic neutron scattering (INS) measurements obtained on the VISION spectrometer were used in conjunction with density functional theory (DFT) calculations performed using VASP to investigate the vibrational lattice dynamics of PCN-250 and provide additional insight into the flexibility of the structure (Figure 5).⁵³⁻⁵⁴ In particular, the spectral features in the region below 150 cm^{-1} were probed as we have previously reported that the low-energy

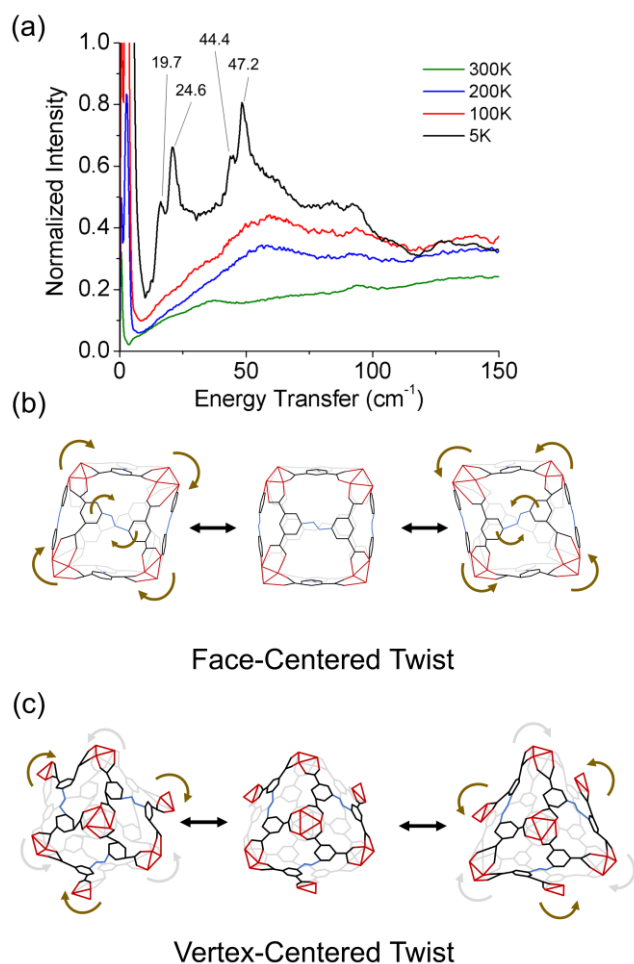


Figure 5. (a) INS spectra of PCN-250-Al. Two particular vibrational modes are highlighted at (b) 19.75 cm^{-1} involving a face-centered twisting motion which deforms the void space within the framework and at (c) 44.43 cm^{-1} involving a vertex-centered twist around the clusters of the framework which compresses and expands the void space.

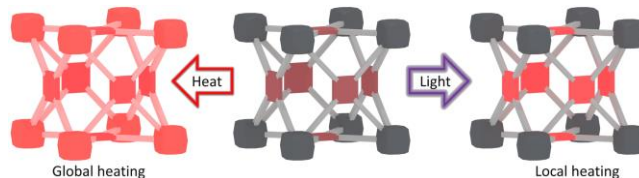


Figure 6. Proposed schematic representing the localized heating phenomena in Type-3 LISA systems such as PCN-250-M.

collective modes are explicitly linked to framework elasticity and mechanisms of instability.⁵⁵⁻⁵⁷ Two particular vibrational modes of interest are highlighted in Figure 5b and c, involving symmetric framework face-centered twist (19.75 cm^{-1}) and vertex-centered twist (44.43 cm^{-1}), respectively. The vertex-centered twisting motion is of particular interest as it resembles the structural deformation of PCN-250 under external pressure.⁵⁸⁻⁵⁹

From the vibrational results, it is possible to see three primary types of ligand vibrations that potentially play a role in the LISA effect, namely in-plane and out-of-plane rotation and out-of-plane bending (Figure S33-35). While the two in-plane and out-of-plane rotations mainly affect the phenyl ring in the ligand, the out-of-plane ligand bending may contribute to the LISA effect as it involves the N=N bond to a greater extent and changes the pore area where host-guest interactions primarily occur. Furthermore, a similar bending dynamic is seen in the single crystal data observed under UV light.

Proposed mechanism of Metal Identity Influence

Azobenzene molecules are known to undergo isomerization in a free solution going from a trans (thermally favored) to a cis-state (electronic excitation favored) in the presence of UV light.³² The exact wavelength of this transition depends upon the functional group attachments on the phenyl portion of azobenzene. As the electron-withdrawing and donating features change, the absorption maximum is either red or blue shifted.^{28, 33-34, 60} When introduced into a framework where both ends of the azobenzene are fixed within the scaffold, the isomerization can no longer occur. An electronically induced thermal relaxation through vibrationally induced 'localized heating' occurs across the N=N bond observed in our SCXRD data (Figure 6). Suppressed localized displacement has been suggested in other reports⁵² as a key feature of the LISA effect and further supported here through the crystallographic calibration curve of U_{11} . The degree of orbital interaction between the metal centers and the azobenzene unit during this electronic-induced thermal relaxation is a key feature, as evident by the gas adsorption performance differences of the PCN-250-M isomorphs. A high degree of interaction with the metal centers, resulting from the overlap between the π bond of the ligand and the metal, resulting in varying dispersions of the electronic energy between the metal center and the azo bond, altering the extent of the LISA effect. In this system, low levels of metal interaction concentrate this energy into the vibrational modes of the azo bond, increasing the thermal effect observed for the LISA system. This is especially apparent in the p-block metal Al, where no readily accessible d-orbital can engage in easy orbital overlap with the ligand π^* after

excitation. Transversely, metal centers with more favorable overlap, such as Fe, can act as electronic energy sinks at the cluster sites through ligand-to-metal electronic transfer, thus reducing the available energy for LISA. Thus, the choice of metal center identity is a crucial feature for the LISA effect in isostructural systems, with the degree of orbital overlap between the ligand and metal generating a higher or lower observed LISA effect.

Conclusion

We have investigated the light-induced switchable adsorption (LISA) phenomena within an isorecticular series of azobenzene-based metal-organic framework (MOF) materials. The mechanism of the LISA effect was studied using single-crystal X-ray diffraction (SCXRD) of both the standard material and under UV-light excitation, with the results showing that the origins of the LISA effect occur through the localized N=N bond of the azobenzene-based linker thermally altering the host-gas interactions resulting in vibrationally induced 'localized heating'. The effects of modifying the metal identity and the accessible orbitals for electronic energy dispersion were also investigated. The results showed a dramatic difference in efficiency dependent on the metal cluster involved with the greatest LISA effect present for the PCN-250-Al structure. Furthermore, the LISA systems' influence on methane (CH₄) and carbon dioxide (CO₂) adsorption at both near ambient and high-pressure systems showed a noticeable reduction in adsorption upon UV-irradiation, indicating its usability for increasing the deliverable working capacity of the materials. The results demonstrate an alternative approach to increasing the working capacity of gas release, especially under high pressure. Finally, the phenomena of light-induced localized heating could provide a groundbreaking alternative approach to traditional thermal regeneration of porous materials for gas release.

AUTHOR INFORMATION

Corresponding Authors

* rydermr@ornl.gov; zhou@chem.tamu.edu to whom correspondence should be addressed.

Author Contributions

The manuscript was written through the contributions of all authors, and all authors have approved the final version.

SUPPORTING INFORMATION

Experimental procedures and data are in the supporting information, and the accompanying single-crystal data are supporting CIF files.

ACKNOWLEDGMENT

H.F.D., G.S.D., and M.R.R. acknowledge the U.S. Department of Energy (DOE) Office of Science Graduate Student Research (SCGSR) program for funding. The SCGSR program is administered by the Oak Ridge Institute for Science and Education (ORISE) for the DOE under contract number DE-SC0014664. M.R.R. also acknowledges the DOE Office of Science (Basic Energy Sciences) and DOE Office of Fossil Energy and Carbon

Management for additional research funding and the National Energy Research Scientific Computing Center (NERSC), a DOE Office of Science User Facility operated under Contract No. DE-AC02-05CH11231 for access to supercomputing resources. H.-C.Z. acknowledges the Robert A. Welch Foundation for a Welch Endowed Chair (A-0030), the financial support of the Qatar National Research Fund award NPRP9-377-1-080, and the Center for Gas Separations Relevant to Clean Energy Technologies, an Energy Frontier Research Center funded by the DOE Office of Science (Basic Energy Sciences) under Contract Number DE-SC0001015. In addition, the authors acknowledge the Texas A&M X-ray Diffraction Laboratory and the NMR User Facility and Dr. Paul A. Lindahl for his contributions to the Mossbauer studies. H. F. D. would also like to thank the FYP Chemistry Program at Texas A&M University and Dr. Edward Lee for access to equipment. This research used resources at the Spallation Neutron Source (SNS), a DOE Office of Science User Facility operated by Oak Ridge National Laboratory, and the Advanced Light Source (ALS), a DOE Office of Science User Facility operated under contract no. DE-AC02-05CH11231 by Lawrence Berkeley National Laboratory.

ABBREVIATIONS

MOF: Metal-Organic Framework

LISA: Light-Induced Switchable Adsorption

UV: Ultra-Violet

MIL: Materials Institut Lavoisier

PCN: Porous Coordination Network

TGA-MS: Thermogravimetric analysis- Mass Spectrometry

ABTC: 3,3',5,5'-azobenzene tetracarboxylic acid

PXRD: Powder X-ray Diffraction

SCXRD: Single Crystal X-ray Diffraction

CO₂: Carbon Dioxide

CH₄: Methane

ADP: Atomic Displacement Parameter

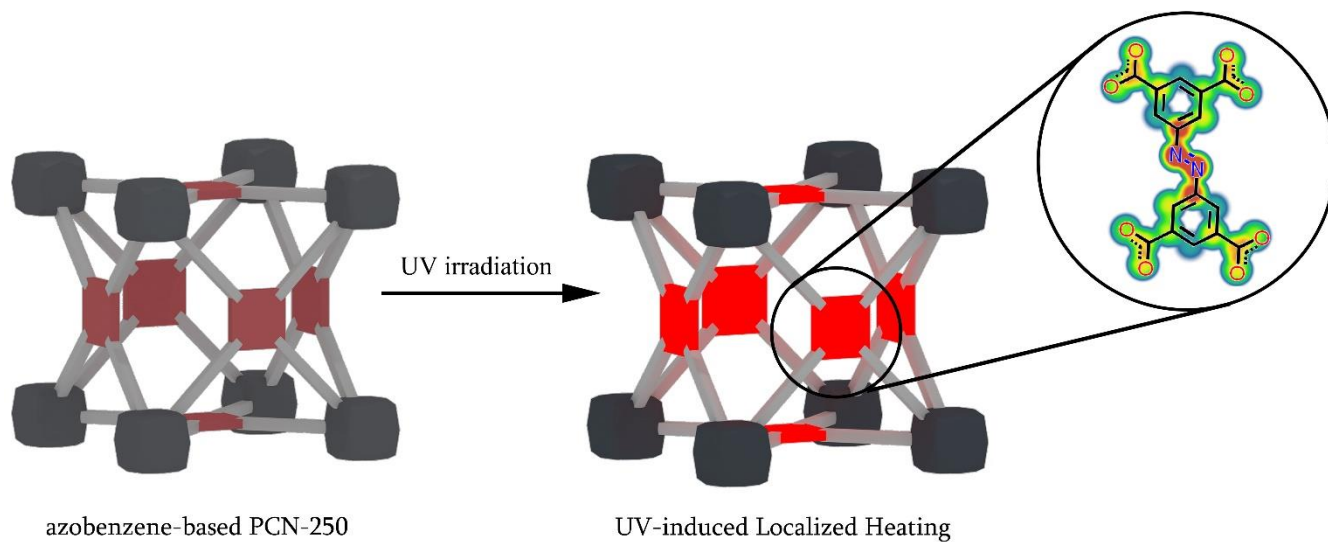
REFERENCES

1. Wegrzyn, J.; Gurevich, M., Adsorbent storage of natural gas. *Applied Energy* **1996**, *55* (2), 71-83.
2. Lee, S.-J.; Bae, Y.-S., Can Metal-Organic Frameworks Attain New DOE Targets for On-Board Methane Storage by Increasing Methane Heat of Adsorption? *The Journal of Physical Chemistry C* **2014**, *118* (34), 19833-19841.
3. Sumida, K.; Rogow, D. L.; Mason, J. A.; McDonald, T. M.; Bloch, E. D.; Herm, Z. R.; Bae, T. H.; Long, J. R., Carbon dioxide capture in metal-organic frameworks. *Chem Rev* **2012**, *112* (2), 724-81.
4. Gomez-Gualdrón, D. A.; Gutov, O. V.; Krungleviciute, V.; Borah, B.; Mondloch, J. E.; Hupp, J. T.; Yildirim, T.; Farha, O. K.; Snurr, R. Q., Computational Design of Metal-Organic Frameworks Based on Stable Zirconium Building Units for Storage and Delivery of Methane. *Chem Mater* **2014**, *26* (19), 5632-5639.
5. Duren, T.; Sarkisov, L.; Yaghi, O. M.; Snurr, R. Q., Design of new materials for methane storage. *Langmuir* **2004**, *20* (7), 2683-9.
6. Day, G. S.; Drake, H. F.; Zhou, H.-C.; Ryder, M. R., Evolution of porous materials from ancient remedies to modern frameworks. *Communications Chemistry* **2021**, *4* (1), 114.
7. Furukawa, H.; Cordova, K. E.; O'Keeffe, M.; Yaghi, O. M., The chemistry and applications of metal-organic frameworks. *Science* **2013**, *341* (6149), 1230444.

8. Yu, J.; Xie, L. H.; Li, J. R.; Ma, Y.; Seminario, J. M.; Balbuena, P. B., CO₂ Capture and Separations Using MOFs: Computational and Experimental Studies. *Chem Rev* **2017**, *117* (14), 9674-9754.
9. Kirchon, A.; Feng, L.; Drake, H. F.; Joseph, E. A.; Zhou, H. C., From fundamentals to applications: a toolbox for robust and multifunctional MOF materials. *Chem Soc Rev* **2018**, *47* (23), 8611-8638.
10. Hendon, C. H.; Rieth, A. J.; Korzynski, M. D.; Dinca, M., Grand Challenges and Future Opportunities for Metal-Organic Frameworks. *ACS Cent Sci* **2017**, *3* (6), 554-563.
11. U.S. Energy Information Administration (EIA), Monthly Energy Review, DOE/EIA - 0035(2020/4), April 2020.
12. Lee, S.-J.; Bae, Y.-S., Can Metal-Organic Frameworks Attain New DOE Targets for On-Board Methane Storage by Increasing Methane Heat of Adsorption? *J. Phys. Chem. C* **2014**, *118* (34), 19833-19841.
13. Chen, Z.; Li, P.; Anderson, R.; Wang, X.; Zhang, X.; Robison, L.; Redfern, L. R.; Moribe, S.; Islamoglu, T.; Gomez-Gualdrón, D. A.; Yildirim, T.; Stoddart, J. F.; Farha, O. K., Balancing volumetric and gravimetric uptake in highly porous materials for clean energy. *Science* **2020**, *368* (6488), 297-303.
14. Gomez-Gualdrón, D. A.; Wilmer, C. E.; Farha, O. K.; Hupp, J. T.; Snurr, R. Q., Exploring the Limits of Methane Storage and Delivery in Nanoporous Materials. *Journal of Physical Chemistry C* **2014**, *118* (13), 6941-6951.
15. Huang, P.; Chen, C.; Hong, Z.; Pang, J.; Wu, M.; Jiang, F.; Hong, M., Azobenzene Decorated NbO-Type Metal-Organic Framework for High-Capacity Storage of Energy Gases. *Inorg Chem* **2019**, *58* (18), 11983-11987.
16. Farha, O. K.; Yazaydin, A. O.; Eryazici, I.; Malliakas, C. D.; Hauser, B. G.; Kanatzidis, M. G.; Nguyen, S. T.; Snurr, R. Q.; Hupp, J. T., De novo synthesis of a metal-organic framework material featuring ultrahigh surface area and gas storage capacities. *Nat Chem* **2010**, *2* (11), 944-8.
17. Liang, C. C.; Shi, Z. L.; He, C. T.; Tan, J.; Zhou, H. D.; Zhou, H. L.; Lee, Y.; Zhang, Y. B., Engineering of Pore Geometry for Ultrahigh Capacity Methane Storage in Mesoporous Metal-Organic Frameworks. *J Am Chem Soc* **2017**, *139* (38), 13300-13303.
18. Mason, J. A.; Veenstra, M.; Long, J. R., Evaluating metal-organic frameworks for natural gas storage. *Chem Sci* **2014**, *5* (1), 32-51.
19. Gomez-Gualdrón, D. A.; Colon, Y. J.; Zhang, X.; Wang, T. C.; Chen, Y. S.; Hupp, J. T.; Yildirim, T.; Farha, O. K.; Zhang, J.; Snurr, R. Q., Evaluating topologically diverse metal-organic frameworks for cryo-adsorbed hydrogen storage. *Energ Environ Sci* **2016**, *9* (10), 3279-3289.
20. Gong, L.; Feng, X. F.; Luo, F., Novel azo-Metal-Organic Framework Showing a 10-Connected bct Net, Breathing Behavior, and Unique Photoswitching Behavior toward CO₂. *Inorg Chem* **2015**, *54* (24), 11587-9.
21. Alhamami, M.; Doan, H.; Cheng, C. H., A Review on Breathing Behaviors of Metal-Organic-Frameworks (MOFs) for Gas Adsorption. *Materials (Basel)* **2014**, *7* (4), 3198-3250.
22. Serre, C.; Millange, F.; Thouvenot, C.; Nogues, M.; Marsolier, G.; Louer, D.; Férey, G., Very large breathing effect in the first nanoporous chromium(III)-based solids: MIL-53 or Cr(III)(OH) x [O(2)C-C(6)H(4)-CO(2)] x [HO(2)C-C(6)H(4)-CO(2)H](x) x H(2)O(y). *J Am Chem Soc* **2002**, *124* (45), 13519-26.
23. Connolly, B. M.; Madden, D. G.; Wheatley, A. E. H.; Fairen-Jimenez, D., Shaping the Future of Fuel: Monolithic Metal-Organic Frameworks for High-Density Gas Storage. *J Am Chem Soc* **2020**, *142* (19), 8541-8549.
24. Yu, M. H.; Space, B.; Franz, D.; Zhou, W.; He, C.; Li, L.; Krishna, R.; Chang, Z.; Li, W.; Hu, T. L.; Bu, X. H., Enhanced Gas Uptake in a Microporous Metal-Organic Framework via a Sorbate Induced-Fit Mechanism. *J Am Chem Soc* **2019**, *141* (44), 17703-17712.
25. Lyndon, R.; Konstas, K.; Ladewig, B. P.; Southon, P. D.; Kepert, P. C.; Hill, M. R., Dynamic photo-switching in metal-organic frameworks as a route to low-energy carbon dioxide capture and release. *Angew Chem Int Ed Engl* **2013**, *52* (13), 3695-8.
26. Huang, X. H.; Li, T., Recent progress in the development of molecular-scale electronics based on photoswitchable molecules. *Journal of Materials Chemistry C* **2020**, *8* (3), 821-848.
27. Xiao, Z.; Drake, H. F.; Rezenom, Y. H.; Cai, P.; Zhou, H.-C., Structural Manipulation of a Zirconocene-based Porous Coordination Cage Using External and Host-Guest Stimuli. *Small Structures n/a* (n/a).
28. Hermann, D.; Schwartz, H. A.; Werker, M.; Schaniel, D.; Ruschewitz, U., Metal-Organic Frameworks as Hosts for Fluorinated Azobenzenes: A Path towards Quantitative Photoswitching with Visible Light. *Chemistry* **2019**, *25* (14), 3606-3616.
29. Hermann, D.; Emerich, H.; Lepski, R.; Schaniel, D.; Ruschewitz, U., Metal-organic frameworks as hosts for photochromic guest molecules. *Inorg Chem* **2013**, *52* (5), 2744-9.
30. Brown, J. W.; Henderson, B. L.; Kiesz, M. D.; Whalley, A. C.; Morris, W.; Grunder, S.; Deng, H. X.; Furukawa, H.; Zink, J. I.; Stoddart, J. F.; Yaghi, O. M., Photophysical pore control in an azobenzene-containing metal-organic framework. *Chem Sci* **2013**, *4* (7), 2858-2864.
31. Fan, C. B.; Liu, Z. Q.; Gong, L. L.; Zheng, A. M.; Zhang, L.; Yan, C. S.; Wu, H. Q.; Feng, X. F.; Luo, F., Photoswitching adsorption selectivity in a diarylethene-azobenzene MOF. *Chem Commun (Camb)* **2017**, *53* (4), 763-766.
32. Kumar, G. S.; Neckers, D. C., Photochemistry of Azobenzene-Containing Polymers. *Chemical Reviews* **1989**, *89* (8), 1915-1925.
33. Muller, K.; Knebel, A.; Zhao, F.; Bleger, D.; Caro, J.; Heinke, L., Switching Thin Films of Azobenzene-Containing Metal-Organic Frameworks with Visible Light. *Chemistry* **2017**, *23* (23), 5434-5438.
34. Zhang, Z.; Muller, K.; Heidrich, S.; Koenig, M.; Hashem, T.; Schloder, T.; Bleger, D.; Wenzel, W.; Heinke, L., Light-Switchable One-Dimensional Photonic Crystals Based on MOFs with Photomodulatable Refractive Index. *J Phys Chem Lett* **2019**, *10* (21), 6626-6633.
35. He, J.; Aggarwal, K.; Katyal, N.; He, S.; Chiang, E.; Dunning, S. G.; Reynolds, J. E., 3rd; Steiner, A.; Henkelman, G.; Que, E. L.; Humphrey, S. M., Reversible Solid-State Isomerism of Azobenzene-Loaded Large-Pore Isorecticular Mg-CUK-1. *J Am Chem Soc* **2020**, *142* (14), 6467-6471.
36. Yanai, N.; Uemura, T.; Inoue, M.; Matsuda, R.; Fukushima, T.; Tsujimoto, M.; Isoda, S.; Kitagawa, S., Guest-to-host transmission of structural changes for stimuli-

- responsive adsorption property. *J Am Chem Soc* **2012**, *134* (10), 4501-4.
37. Meng, X.; Gui, B.; Yuan, D.; Zeller, M.; Wang, C., Mechanized azobenzene-functionalized zirconium metal-organic framework for on-command cargo release. *Sci Adv* **2016**, *2* (8), e1600480.
38. Knebel, A.; Sundermann, L.; Mohmeyer, A.; Strauss, I.; Friebe, S.; Behrens, P.; Caro, J., Azobenzene Guest Molecules as Light-Switchable CO₂ Valves in an Ultrathin UiO-67 Membrane. *Chemistry of Materials* **2017**, *29* (7), 3111-3117.
39. Park, J.; Yuan, D.; Pham, K. T.; Li, J. R.; Yakovenko, A.; Zhou, H. C., Reversible alteration of CO₂ adsorption upon photochemical or thermal treatment in a metal-organic framework. *J Am Chem Soc* **2012**, *134* (1), 99-102.
40. Li, H.; Sadiq, M. M.; Suzuki, K.; Ricco, R.; Doblin, C.; Hill, A. J.; Lim, S.; Falcaro, P.; Hill, M. R., Magnetic Metal-Organic Frameworks for Efficient Carbon Dioxide Capture and Remote Trigger Release. *Adv Mater* **2016**, *28* (9), 1839-44.
41. Li, H. Q.; Sadiq, M. M.; Suzuki, K.; Doblin, C.; Lim, S.; Falcaro, P.; Hill, A. J.; Hill, M. R., MaLISA - a cooperative method to release adsorbed gases from metal-organic frameworks. *J Mater Chem A* **2016**, *4* (48), 18757-18762.
42. Dhakshinamoorthy, A.; Alvaro, M.; Chevreau, H.; Horcajada, P.; Devic, T.; Serre, C.; Garcia, H., Iron(iii) metal-organic frameworks as solid Lewis acids for the isomerization of α -pinene oxide. *Catal. Sci. Technol.* **2012**, *2* (2), 324-330.
43. Drake, H. F.; Xiao, Z.; Day, G. S.; Vali, S. W.; Chen, W.; Wang, Q.; Huang, Y.; Yan, T.-H.; Kuszynski, J. E.; Lindahl, P. A.; Ryder, M. R.; Zhou, H.-C., Thermal decarboxylation for the generation of hierarchical porosity in isostructural metal-organic frameworks containing open metal sites. *Materials Advances* **2021**, *2* (16), 5487-5493.
44. Kirchon, A.; Zhang, P.; Li, J.; Joseph, E. A.; Chen, W.; Zhou, H.-C., Effect of Isomorphic Metal Substitution on the Fenton and Photo-Fenton Degradation of Methylene Blue Using Fe-Based Metal-Organic Frameworks. *ACS Applied Materials & Interfaces* **2020**, *12* (8), 9292-9299.
45. Belmabkhout, Y.; Pillai, R. S.; Alezi, D.; Shekhah, O.; Bhatt, P. M.; Chen, Z.; Adil, K.; Vaesen, S.; De Weireld, G.; Pang, M.; Suetin, M.; Cairns, A. J.; Solovyeva, V.; Shkurenko, A.; El Tall, O.; Maurin, G.; Eddaoudi, M., Metal-organic frameworks to satisfy gas upgrading demands: fine-tuning the soc-MOF platform for the operative removal of H₂S. *J. Mater. Chem. A* **2017**, *5* (7), 3293-3303.
46. Yuan, S.; Sun, X.; Pang, J.; Lollar, C.; Qin, J.-S.; Perry, Z.; Joseph, E.; Wang, X.; Fang, Y.; Bosch, M.; Sun, D.; Liu, D.; Zhou, H.-C., PCN-250 under Pressure: Sequential Phase Transformation and the Implications for MOF Densification. *Joule* **2017**, *1* (4), 806-815.
47. Liu, Y.; Eubank, J. F.; Cairns, A. J.; Eckert, J.; Kravtsov, V. C.; Luebke, R.; Eddaoudi, M., Assembly of Metal-Organic Frameworks (MOFs) Based on Indium-Trimer Building Blocks: A Porous MOF with soc Topology and High Hydrogen Storage. *Angewandte Chemie International Edition* **2007**, *46* (18), 3278-3283.
48. Mowat, J. P. S.; Miller, S. R.; Slawin, A. M. Z.; Seymour, V. R.; Ashbrook, S. E.; Wright, P. A., Synthesis, characterisation and adsorption properties of microporous scandium carboxylates with rigid and flexible frameworks. *Microporous and Mesoporous Materials* **2011**, *142* (1), 322-333.
49. Drake, H. F.; Day, G. S.; Vali, S. W.; Xiao, Z.; Banerjee, S.; Li, J.; Joseph, E. A.; Kuszynski, J. E.; Perry, Z. T.; Kirchon, A.; Ozdemir, O. K.; Lindahl, P. A.; Zhou, H. C., The thermally induced decarboxylation mechanism of a mixed-oxidation state carboxylate-based iron metal-organic framework. *Chem Commun (Camb)* **2019**, *55* (85), 12769-12772.
50. Nelson, A. P.; Farha, O. K.; Mulfort, K. L.; Hupp, J. T., Supercritical processing as a route to high internal surface areas and permanent microporosity in metal-organic framework materials. *J Am Chem Soc* **2009**, *131* (2), 458-60.
51. Thommes, M.; Kaneko, K.; Neimark, A. V.; Olivier, J. P.; Rodriguez-Reinoso, F.; Rouquerol, J.; Sing, K. S. W., Physisorption of gases, with special reference to the evaluation of surface area and pore size distribution (IUPAC Technical Report). *Pure Appl Chem* **2015**, *87* (9-10), 1051-1069.
52. Li, H.; Martinez, M. R.; Perry, Z.; Zhou, H. C.; Falcaro, P.; Doblin, C.; Lim, S.; Hill, A. J.; Halstead, B.; Hill, M. R., A Robust Metal-Organic Framework for Dynamic Light-Induced Swelling Adsorption of Carbon Dioxide. *Chemistry* **2016**, *22* (32), 11176-9.
53. Armstrong, J.; O'Malley, A. J.; Ryder, M. R.; Butler, K. T., Understanding dynamic properties of materials using neutron spectroscopy and atomistic simulation. *Journal of Physics Communications* **2020**, *4* (7), 072001.
54. Armstrong, J.; Butler, K. T.; Ryder, M. R., Computers in neutron science. *Journal of Physics Communications* **2020**, *4* (11), 110401.
55. Ryder, M. R.; Civalleri, B.; Bennett, T. D.; Henke, S.; Rudic, S.; Cinque, G.; Fernandez-Alonso, F.; Tan, J. C., Identifying the role of terahertz vibrations in metal-organic frameworks: from gate-opening phenomenon to shear-driven structural destabilization. *Phys Rev Lett* **2014**, *113* (21), 215502.
56. Ryder, M. R.; Van de Voorde, B.; Civalleri, B.; Bennett, T. D.; Mukhopadhyay, S.; Cinque, G.; Fernandez-Alonso, F.; De Vos, D.; Rudic, S.; Tan, J. C., Detecting Molecular Rotational Dynamics Complementing the Low-Frequency Terahertz Vibrations in a Zirconium-Based Metal-Organic Framework. *Phys Rev Lett* **2017**, *118* (25), 255502.
57. Ryder, M. R.; Civalleri, B.; Cinque, G.; Tan, J.-C., Discovering connections between terahertz vibrations and elasticity underpinning the collective dynamics of the HKUST-1 metal-organic framework. *CrystEngComm* **2016**, *18* (23), 4303-4312.
58. Yuan, S.; Sun, X.; Pang, J. D.; Lollar, C.; Qin, J. S.; Perry, Z.; Joseph, E.; Wang, X.; Fang, Y.; Bosch, M.; Sun, D.; Liu, D. H.; Zhou, H. C., PCN-250 under Pressure: Sequential Phase Transformation and the Implications for MOF Densification. *Joule* **2017**, *1* (4), 806-815.
59. Maul, J.; Ryder, M. R.; Ruggiero, M. T.; Erba, A., Pressure-driven mechanical anisotropy and destabilization in zeolitic imidazolate frameworks. *Physical Review B* **2019**, *99* (1), 014102.
60. Muller, K.; Helfferich, J.; Zhao, F.; Verma, R.; Kanj, A. B.; Meded, V.; Bleger, D.; Wenzel, W.; Heinke, L., Switching the Proton Conduction in Nanoporous, Crystalline Materials by Light. *Adv Mater* **2018**, *30* (8), 1706551.

Image:



Caption:

The mechanism and influencing factors of the UV light-triggered localized thermal response and light-induced switchable adsorption (LISA) are investigated towards carbon dioxide and methane storage.